MINISTÉRIO DA CIÊNCIA, TECNOLOGIA E INOVAÇÕES
INSTITUTO NACIONAL DE PESQUISAS ESPACIAIS

sid.inpe.br/mtc-m21d/2022/05.20.11.14-NTC

THE SEA SURFACE TEMPERATURE DIURNAL CYCLE ROLE IN SUBSEASONAL AND SEASONAL METEOROLOGICAL SYSTEMS

Isabella Talamoni Lima
Paulo Yoshio Kubota
Dayana Castilho de Souza

Technical Note

URL do documento original:
<http://urlib.net/8JMKD3MGP3W34T/46TGJ8P>

INPE
São José dos Campos
2022

PUBLICADO POR:

Instituto Nacional de Pesquisas Espaciais - INPE
Coordenação de Ensino, Pesquisa e Extensão (COEPE)
Divisão de Biblioteca (DIBIB)
CEP 12.227-010
São José dos Campos - SP - Brasil
Tel.:(012) 3208-6923/7348
E-mail: pubtc@inpe.br

MINISTÉRIO DA CIÊNCIA, TECNOLOGIA E INOVAÇÕES
INSTITUTO NACIONAL DE PESQUISAS ESPACIAIS

sid.inpe.br/mtc-m21d/2022/05.20.11.14-NTC

THE SEA SURFACE TEMPERATURE DIURNAL CYCLE ROLE IN SUBSEASONAL AND SEASONAL METEOROLOGICAL SYSTEMS

Isabella Talamoni Lima
Paulo Yoshio Kubota
Dayana Castilho de Souza

Technical Note

URL do documento original:
<http://urlib.net/8JMKD3MGP3W34T/46TGJ8P>

INPE
São José dos Campos
2022

ABSTRACT

The diurnal warming or Sea Surface Temperature (SST) diurnal cycle is a mode of variation that has been receiving more attention through the years. It plays an important role in the ocean-atmosphere interaction because it modulates the air-sea exchange at the interface, including energy (latent and sensible heat), mass (water and trace gases) and momentum fluxes. Although the global annual SST diurnal cycle amplitude (dSST) average is 0.1°C, over regions with strong incident radiation and weak winds the dSST can reach values higher than 5°C. The diurnal energy is stored in the Ocean Mixed Layer (OML) and interacts with daily, intraseasonal and seasonal meteorological scales through SST variability. However, the SST diurnal cycle is poorly represented or parameterized in most numerical weather predictions and climate studies. Therefore, this document explores the efforts made to understand and represent the SST diurnal cycle and how it can affect seasonal and subseasonal meteorological systems.

Keywords: Sea Surface Temperature. Diurnal Cycle. Ocean-Atmosphere Interaction. Subseasonal. Seasonal. Ocean Mixed Layer.

O PAPEL DO CICLO DIURNO DA TEMPERATURA DA SUPERFÍCIE DO MAR EM SISTEMAS METEOROLÓGICOS SUBSAZONAIS E SAZONAIS

RESUMO

O aquecimento diurno ou ciclo diurno da Temperatura da Superfície do Mar (SST) é é um modo de variabilidade que vem recebendo atenção ao longo dos anos. Este ciclo exerce um papel importante na interação oceano-atmosfera porque modula as trocas ar-mar que ocorrem na interface, incluindo os fluxos de energia (calor sensível e latente), de massa (água e gases traço) e de momentum. Embora a média global da amplitude do ciclo diurno da SST (dSST) seja de O.1°C, em regiões com forte radiação incidente e ventos fracos, a dSST pode atingir valores superiores a 5°C. A energia do ciclo diurno é armazenada na Camada Limite Oceânica (OML) e interage com as escalas meteorológicas diurna, subsazonal e sazonal por meio da variablidade da SST. Apesar disso, o ciclo diurno da SST ainda não é bem representado ou parametrizado na maioria dos estudos numéricos de precisão de tempo e clima. Portanto, este documento buscou explorar os esforços feitos para entender e representar o ciclo diurno da SST e como este pode afetar os sistemas meteorológicos subsazonais e sazonais.

LIST OF FIGURES

Page

LIST OF ABBREVIATIONS

AMSR-E	–	Microwave Sesnor Aboard Aqua Satellite
ASCII	–	Air-Sea Convective Intraseasonal Interaction
CF	–	Coupling Frequency
CGCM	–	Coupled General Circulation Model
DWL	–	Diurnal Warm Layer
dSST	–	Sea Surface Temperature Diurnal Cycle Amplitude
ENSO	–	El Niño Southern Oscillation
H	–	Sensible Heat Flux
ISM	–	Indian Summer Monsoon
ITCZ	–	Intertropical Convergence Zone
LE	–	Latent Heat Flux
MABL	–	Marine Atmospheric Boundary Layer
MJO	–	Madden-Julian Oscillation
OGCM	–	Ocean General Circulation Model
OML	–	Ocean Mixed Layer
SST	–	Sea Surface Temperature
SWF	–	Downward Shortwave Flux
SSTint	–	Interface SST
SSTskin	–	Skin SST
SSTsubskin	–	Subskin SST
SSTdepth	–	SST at depth
SSTfnd	–	Foundation SST
S2S	–	Subseasonal to Seasonal Forecasting Project
WISHE	–	Wind Induced Surface Heat Exchange
WCRP	–	World Climate Research Program
WWRP	–	World Weather Research Program

CONTENTS

1 INTRODUCTION

The short to medium-term weather prediction ability depends on the initial conditions of the atmosphere (KALNAY, 2003), and the seasonal climate prediction ability depends on boundary conditions, such as lower boundary conditions from the coupled land-ocean system (SHUKLA, 1998). The subseasonal scale, which lies between the weather and climate scales, is influenced by the initial conditions of the atmosphere and by the slower evolving boundary conditions, such as sea surface temperature (SST), soil moisture and marine ice components, for example (VITART et al., 2012).

The scientific interest in developing numerical models with high subseasonal to seasonal prediction ability has increased, thus, the World Weather Research Program (WWRP) together with the World Climate Research Program (WCRP) implemented the Subseasonal to Seasonal Forecasting Project (Subseasonal to Seasonal; S2S). This project brings together efforts from worldwide Meteorological Centers motivated to fill the gap between weather and climate forecasting (ROBERTSON et al., 2015).

The subseasonal to seasonal prediction ability depends both on realistic boundary conditions and a good representation of the variability modes of the climate system (ANDRADE et al., 2019), which is a great challenge to numerical modelling (CHEN et al., 2010; DOBLAS-REYES et al., 2013). The model ability in representing the evolution of Madden-Julian Oscillation (MJO; Zhang (2005)), for example, has significantly improved in the last decade. The use of coupled models has shown improvements in MJO representation (BERNIE et al., 2007; WOOLNOUGH et al., 2007), which the vertical resolution of the oceanic component was important for its prediction advances associated with the better representation of the SST diurnal cycle (WOOLNOUGH et al., 2007). However, persistent errors are still present in most climate simulations, especially observed in tropical precipitation and cloud cover (COELHO et al., 2021). Some of these errors are produced by the numerical scheme and physical parameterizations and others are due to incorrect representation of the coupled ocean-atmosphere feedbacks (BRUNET et al., 2010).

One of these coupled ocean-atmosphere feedbacks involves the importance of resolving the SST diurnal cycle, which is the daily progression of solar heating and subsequent cooling by mixing in the Ocean Mixed Layer (OML). The SST diurnal cycle is an important feature of ocean-atmosphere interaction because it modulates the air-sea exchange at the interface, including sensible and latent heat fluxes, mois-

ture and trace gases fluxes, and momentum fluxes (KAWAI; WADA, 2007; CLAYSON; BOGDANOFF, 2013). Furthermore, the diurnal energy stored in the OML interacts with daily (JOHNSON et al., 1999; SLINGO et al., 2003; BENEDICT; RANDALL, 2007), intraseasonal (BERNIE et al., 2008; SEO et al., 2014; STAN, 2018) and seasonal (MUJUMDAR et al., 2010; TERRAY et al., 2012; ZHANG et al., 2019) meteorological phenomena. However, the SST diurnal cycle is poorly represented or parameterized in most numerical models (SALISBURY et al., 2018). For this reason, this document discusses the hypothesis that a good representation of the diurnal cycle of SST in coupled models and the energy propagation between diurnal to seasonal scales is essential to obtain a consistent and highly accurate forecast.

2 BIBLIOGRAPHICAL REVIEW

2.1 THE EARTH SYSTEM

Solar radiation is the core driver of the Earth system, which is an integrated system of all the physical, chemical and biological processes within the planet (STEFFEN et al., 2020). The Earth system is often divided into four sub-systems: geosphere, atmosphere, hydrosphere and biosphere (HARTMANN, 2015). The geosphere includes all the rocks and minerals on Earth, from tectonic plates to different soil types and topography. The biosphere includes all the living organisms and their interactions, from plants to humans. The hydrosphere contains all the water in its three-state phases (liquid, gaseous and solid). Usually, the solid (ice) is separated in another sphere, called the cryosphere. Lastly, the atmosphere is the thin layer of mixed gases surrounding the Earth. All these subsystems' processes and interactions are essential to determine the climate, which can be expressed as the mean state of precipitation, temperature, wind, cloud cover, and solar radiation (TRENBERTH, 2002). The climate is an open system due to its mass, energy, and momentum exchanges between the Earth system components aforementioned. Each component contributes to different climate phenomena timescales (HARTMANN, 2015). The oceans and the atmosphere are fluids that transport heat, humidity, and tracers along with the Earth to reduce the differential equator to pole heating (TRENBERTH, 2002). Therefore, here we will focus on the ocean-atmosphere coupling.

2.2 OCEAN AND ATMOSPHERE

Ocean and atmosphere exchange energy (sensible and latent heat fluxes), mass (freshwater and gases) and momentum through the Ocean Mixed Layer (OML) and the Marine Atmospheric Boundary Layer (MABL) interface. The fluxes across this interface, also called air-sea fluxes, are:

a) Sensible Heat Flux (H): exchange of heat energy by conduction or convection. Liu et al. (2010) estimated that the mean H is approximately 8 $W.m^{-2}$ in the upper 50 m over the south-central equatorial Pacific using oceanic reanalysis datasets;

b) Latent Heat Flux (LE): exchange of latent energy associated with water phase changes from the ocean to the atmosphere. A great part of the incoming shortwave energy is used for water phase changes, such as the mean LE is approximately 141 $W.m^{-2}$, also according to Liu et al. (2010)

estimates;

c) Freshwater Flux: exchange of water being part of the water cycle. The oceans are the main water source to the atmosphere in the water cycle (they contribute to more than 80% of water in the atmosphere; (DURACK et al., 2016)). The precipitation also contributes as a freshwater flux from the atmosphere to the ocean (representing 78% of the incoming water flux in the ocean; (DURACK et al., 2016));

d) Gases Flux: exchange of inert and soluble gases such as carbon dioxide (CO_2), oxygen (O_2), methane (CH_4), and nitrous oxide (N_2O). Although the oceans are often mentioned as an important CO2 sink and O_2 source, thus, playing an important role in climate change (ZHONGMING et al., 2021) the climatological mean annual sea-air CO_2 flux shows that the tropical ocean areas are major CO_2 sources to the atmosphere, especially the equatorial Pacific with a seasonally persistent sea-to-air flux of 0.48 Pg-C y^{-1}. On the other hand, a CO_2 sink zone is located between 20–50° latitudes in both hemispheres, associated with strong winds (TAKAHASHI et al., 2009; LANDSCHÜTZER et al., 2020);

e) Momentum Flux: exchange of momentum from the atmosphere circulation to the ocean due to wind stress, generating surface currents, waves, and inducing turbulent mixing in the OML (MOUM; SMYTH, 2001). The wind stress magnitude at the surface ocean can be represented as a function of wind speed, air density, and drag coefficient (KARA et al., 2007).

Pezzi et al. (2005) and Pezzi et al. (2009) investigated whether the MABL can be modulated by strong SST gradients over the Brazil-Malvinas Confluence region. Figure 2.1 shows the temperature profiles of both atmosphere and ocean obtained by in situ observations during the OP23 experiment. In 39°S is verified a strong SST gradient that characterizes the oceanic front. Over warm waters (north of 39°S) a warmer, thicker, unstable and more turbulent MABL was verified. The wind speed was stronger and less vertical shear was also verified. On the other hand, over colder waters (south of 39°S) weak winds but great vertical shear was verified in a colder, thinner, stable and less turbulent MABL.

2.3 OCEAN MIXED LAYER

The OML is the ocean region adjacent to the air–sea interface, which is typically 100 to 150 of metres deep. The OML exchanges chemical, physical and biological

Figure 2.1 - Atmosphere and ocean temperature profiles along with meridional wind vectors over the Brazil-Malvinas Confluence region

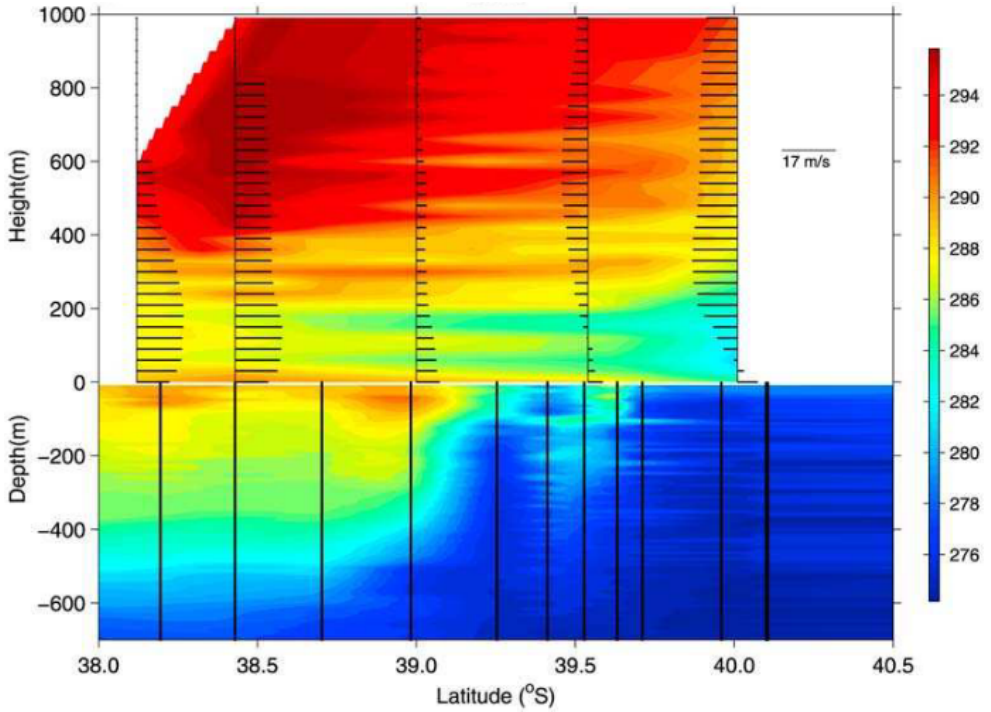

The profiles were taken simultaneously by radiosondes and XBTs along the OSS Ary Rongel's routes during the OP23 experiment OP23 for 3 November 2004.

SOURCE: Pezzi et al. (2009)

properties with MABL, thus, plays an important role in both weather and climate. Figure 2.2 summarizes the coupled ocean-atmosphere processes with a focus on the OML. Number 1 indicates that more than 90% of the incoming solar radiation is absorbed in the first 100 m of the ocean (open ocean mean albedo is 0.06). The solar heating profile in the ocean decreases exponentially with depth. In the first centimetre, infrared radiation is absorbed while blue and green visible wavelengths can penetrate deeper than 100 m. The water's optical properties determine how much of the radiation is absorbed and how deep it can penetrate the ocean. The optical properties depend on the composition, morphology (size and shape of particles), and concentration of the substance dissolved in water (TALLEY, 2011). In turbid coastal waters, the attenuation coefficient can be four times greater than that of pure water, due to the high concentration of phytoplankton and organic matter (TALLEY, 2011). The phytoplankton, for example, absorbs blue and red light during photosynthesis, thus, they attenuate the penetrating sunlight in the ocean (TALLEY, 2011).

Number 2 is showing that the warmer first centimetres of the ocean (skin layer) is cooled by evaporation and air heating, i.e., the available energy is used to evaporate the water (LE) and to heat the adjacent air (H), therefore, both H and LE fluxes are from the ocean to the atmosphere. To balance this energy loss to the atmosphere, upward energy flux is established from the upper ocean layer, right below the skin layer.

While molecular diffusion is the main heat transport mechanism in the first millimetres of the ocean (skin layer), the turbulent mixing, convection, and vertical motion are the heat transport mechanisms in the OML, shown in number 3. These mechanisms are so efficient that the main properties of seawater such as temperature and salinity vary little within the OML depth exemplified by the temperature profile. Right below the OML, the temperature profile experiences a sharp decrease with depth, separating the convective and turbulent layer from the stable and nonturbulent thermocline.

Although the global-average OML depth is about 70 m, however, its depth is associated with the following turbulent mixing processes:

a) Number 4 indicates that the turbulent mixing is mainly driven by the surface wind stress, i.e., the momentum transfer from the wind to the ocean surface feeds the turbulence and generates superficial currents (wind-driven ocean circulation). The wind stress also generates waves on the ocean surface, which can range from capillary waves to wind waves to swell. Breaking waves can disrupt the ocean skin layer and inject bubbles within it, adding turbulent energy, thus increasing the mixing (JANSSEN, 2012);

b) Shown in number 5 is the rate of buoyancy generation that combines heat storage (temperature) and the evaporation-precipitation budget (salinity). It can be depicted by two scenarios: the first involves the cooling of the ocean surface (a fall and winter pattern), thus, cold and dense water near the surface will sink and warm water will rise (convection) and the OML deepens; the second scenario involves a weak cooling or warming of the ocean surface (a spring and summer pattern), thus, warm and lighter water near the surface disfavors the buoyancy generation and a stratified, warm and shallow OML is observed. Besides, the buoyancy generation is also affected by salinity through two main ocean-atmosphere water exchange processes: evaporation and precipitation, the last indicated by number 6.

The saline dense water can balance or even beat the thermal stratification, thus, promoting convection and a deep OML;

c) OML is mixed at the top by the wind (Number 4), waves and buoyancy (Number 5). At the bottom, the entrainment of cold water from below the OML can also contribute to its cooling and deepening shown in Number 7. The vertical entrainment mixes warmer waters in the OML with cooler thermocline waters, thus, deepening the OML. Vertical entrainment is a diabatic process driven by gradients, thus, it can be caused by vertical shear instability from wind-driven horizontal currents, by buoyancy at the sea surface (TALLEY, 2011);

d) Although not shown in Figure 2.2 , Langmuir circulations are also associated with turbulence generation in the OML. These circulations are vortices with axes aligned with the wind direction which can be observed as lines of bubbles or debris (convergence areas between the vortices) on the ocean surface aligned with the wind (MOUM; SMYTH, 2001). These circulations are generated from a horizontal tilt in the vertical relative vorticity of the surface current driven by the shear of the Stokes drift (GRANT; BELCHER, 2009). The turbulence associated with the Langmuir circulation can deepen the OML by intensifying the entrainment of colder water from below the OML (GRANT; BELCHER, 2009);

Therefore, all the mentioned coupled ocean-atmosphere processes contribute to the energy budget on the surface of the ocean, which determines the SST. SST is the main ocean way of forcing the atmosphere, therefore, SST is an important parameter to understand the air-sea fluxes and their feedback mechanisms. The SST for example determines the stability of the upper ocean and by extension dictates the fluxes across the ocean-atmosphere. Some important feedback loops associated with the air-sea fluxes are mentioned below:

a) The freshwater flux feedback loop is associated with the upper ocean salinity budget that also determines the upper ocean stability. The freshwater flux can be from river discharge or precipitation, in either case, it can form a relatively thin freshwater layer right below the OML that stabilizes the water column. It is also called the barrier layer because it inhibits vertical mixing, especially when formed under light winds regime. The barrier layer determines the heat budget in the OML because it blocks the heat

Figure 2.2 - Scheme of the main coupled ocean-atmosphere processes associated with the OML.

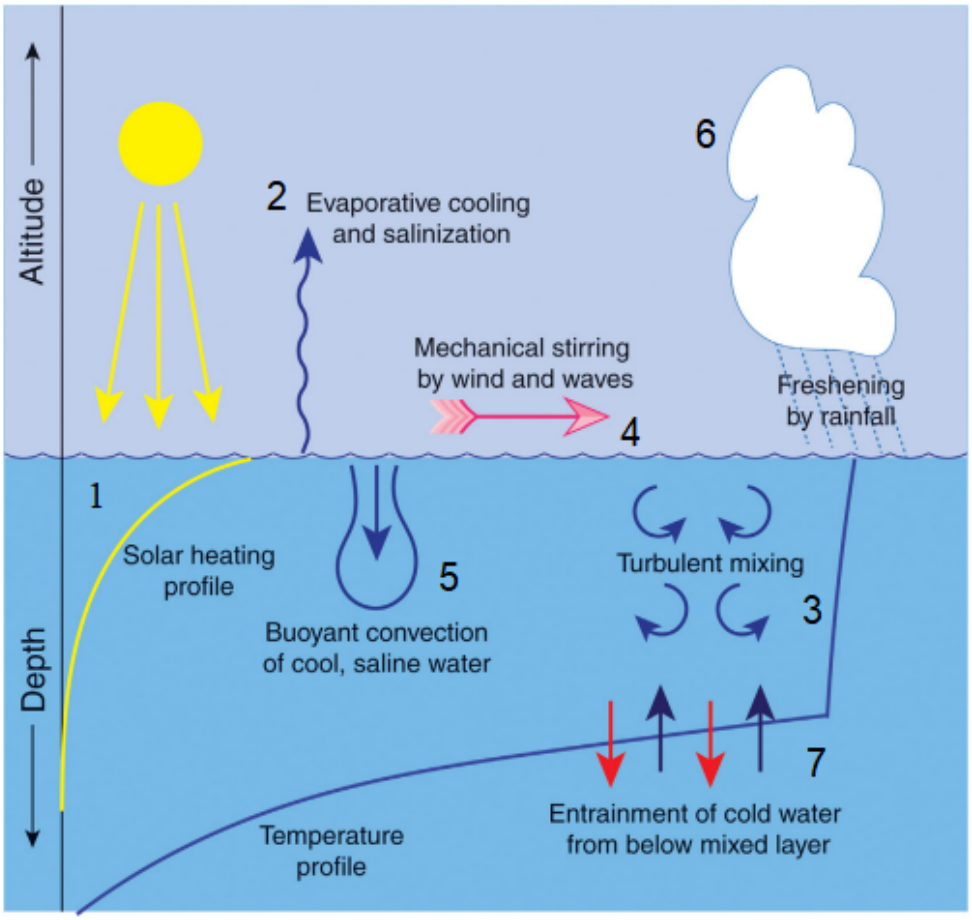

SOURCE: Adapted from Hartmann (2015)

exchange from the surface to deeper layers (GEORGE et al., 2019). Thus, the air-sea fluxes between OML and MABL can be intensified (MISRA, 2020). The potential effect of barrier layer formation on tropical cyclone activity has been studied over the northwestern tropical Atlantic Ocean. Balaguru et al. (2012) verified an increase in tropical cyclones' intensity when they passed through a barrier layer region. The authors suggested that the heat trapped in the layers above (OML and skin) the barrier layer can maintain stronger air-sea fluxes. Barrier layers were also verified over the tropical Atlantic associated with the precipitation of the Intertropical Convergence Zone by Foltz e McPhaden (2009). More recently, Rosa (2022) identified a barrier layer under the maximum precipitation region associated with the Oceanic South Atlantic Convergence Zone which had an influence on

the OML entrainment;

b) The SST, cloud, and radiation interaction is another air-sea feedback that involves a reinforcement between stratiform clouds formed over the ocean surface and SST anomalies. Over the North Pacific during boreal summer, Norris et al. (1998) verified that marine stratiform clouds affect the energy budget at the ocean surface because the low albedo reflects more incoming shortwave radiation, thus, less radiation reaches the ocean surface and the OML cools down. The authors estimated that for a cloud albedo of 35%, each 1% cloud cover increase is able to reduce $1 W.m^{-2}$ of energy on the ocean surface. On the other hand, the SST reduction can influence the cloud cover, especially the marine stratiform clouds. Klein e Hartmann (1993) verified that an air temperature reduction of 0.2K can increase by 1% the marine stratiform clouds. Therefore, SST reduction due to radiation blocking by cloud cover also reinforces the cloud cover increase by promoting a cooling in the MABL over warm waters (NORRIS et al., 1998);

c) The positive feedback between energy fluxes (sensible and latent) and wind speed is defined by air-sea feedback, where the energy fluxes and wind speed have a positive correlation, but the SST decreases. This feedback is part of the Wind Induced Surface Heat Exchange (WISHE; Emanuel (1986) phenomenon that is observed in mesoscale systems such as tropical cyclones (CHENG; WU, 2020).

2.4 SST DIURNAL CYCLE

The SST diurnal cycle or diurnal warming was first reported by Sverdrup et al. (1942) as being essential to studying the air-sea interactions. The diurnal variation of SST observed in the OML is explained by the differential day and night heating (insolation) and by mixing processes. Considering a low wind speed and clear sky conditions, an idealized SST diurnal cycle can be proposed, shown in Figure 2.3a. In the early morning (6 to 7 am) the downward shortwave flux (SWF; Figure 2.3b) promotes a sharp decrease of the OML depth (Figure 2.3c). After a few hours, the heating due to the SWF penetration builds up the OML stratification (shallow OML; Figure 2.3c), i.e., a more stable and less turbulent layer. The SST diurnal cycle peaks in the early afternoon, approximately 2 pm, after the SWF peak and before the OML begins to deepen due to vertical mixing.

Along the afternoon, SWF reduces and the OML becomes more turbulent, i.e., the

energy absorbed during the day is mixed within a deeper OML, because the water near the surface becomes denser (cools) forming convective plumes of rising and sinking plumes (convectively driven mixing). During the night, the surface cooling leads to a stronger mixing (less stratified and unstable layer) which deepens the OML. This stratification reduction during the night promotes a neutral start for the following day cycle.

Figure 2.3 - Idealized SST diurnal cycle explained by the daily SWF and OML mixing variation.

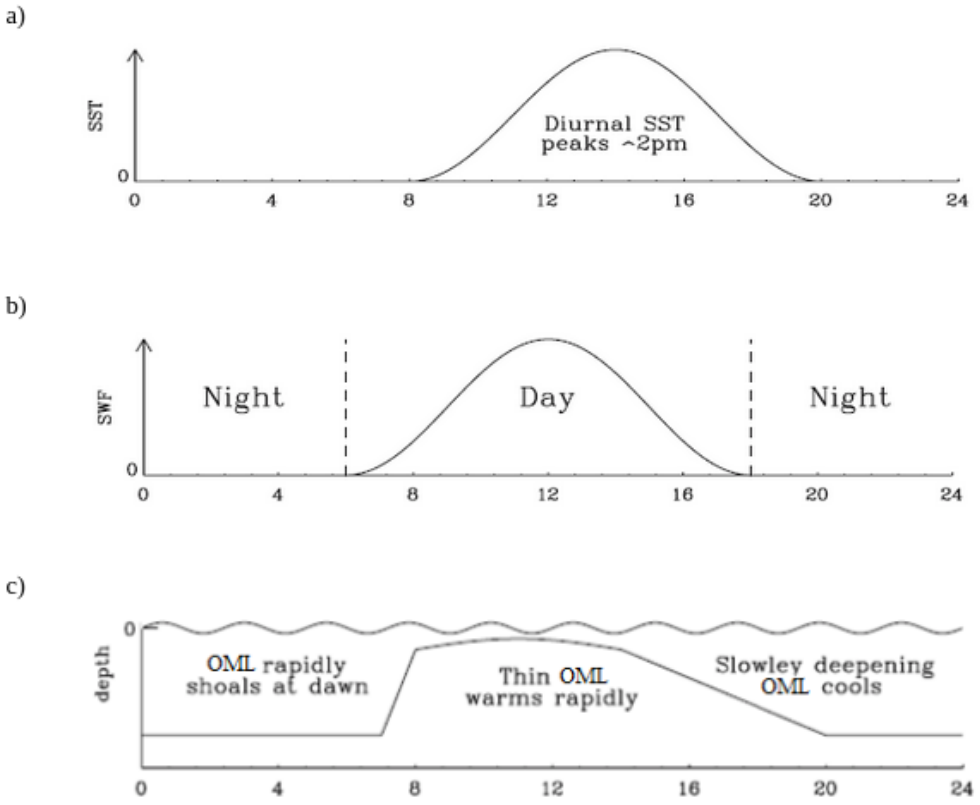

SOURCE: Adapted from Bernie et al. (2007)

The studies often consider the SST diurnal cycle by its amplitude (dSST), defined as the difference between the daily maximum and minimum SST values. Wenegrat e McPhaden (2015) used atmosphere and ocean data from the central equatorial Atlantic (0° and 23°W) PIRATA mooring to obtain the SST diurnal cycle composite from 7 January to 24 May 2009. Figure 2.4a shows the SWF variation with peak at 1200 LT (similar to Figure 2.2b) and Figure 2.4b shows the dSST under light wind condition (Figure 2.4c). The dSST peak was verified at 1400 LT when the

temperature anomaly reached 0.5°C and the layer is stratified, stable and thin shown by the dashed line in Figure 2.4c.

Figure 2.4 - Composite diurnal cycle of SWF (a), dSST (b), temperature anomaly, wind and current shear (c) under light wind conditions.

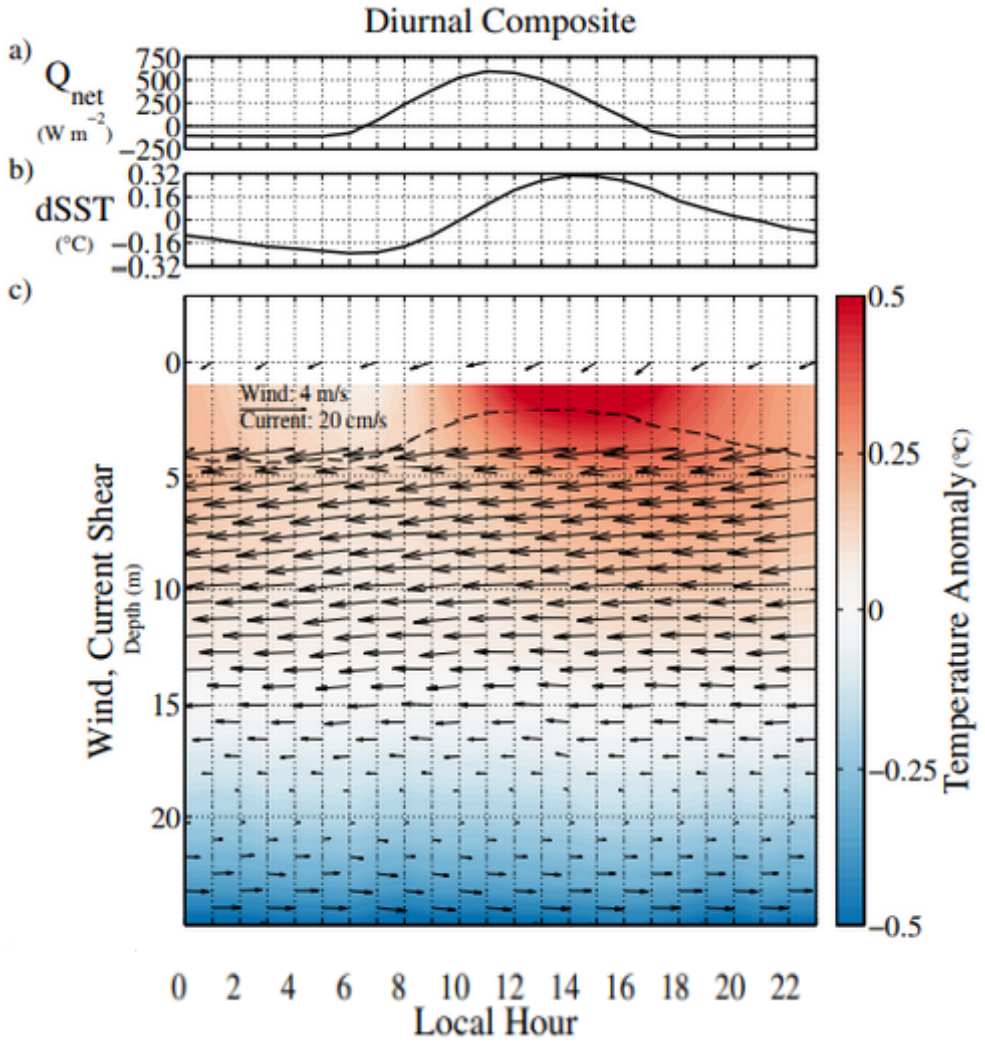

The wind vectors were plotted for z=0 and current vectors at their observation depths. The dashed line shows the OML.

SOURCE: Adapted from Wenegrat e McPhaden (2015)

The SST diurnal cycle magnitude is determined by both oceanographic and meteorological processes that affect the OML stratification. These processes include the SWF (mainly affected by cloud cover), wind speed, temperature, salinity and optical properties of the water column, and vertical mixing processes. Webster et al. (1996)

studied the relation between dSST and the meteorological conditions (Figure 2.5) and showed that:

a) the greatest insolation increases dSST;

b) low wind speed also increases dSST, if the wind speed is equal to or greater than 10 m.s^{-1}, the dSST is zero;

c) precipitation is associated with OML cooling, therefore increasing dSST (a fresh and stable layer is established at the surface, allowing greater surface heating).

Figure 2.5 - The diurnal amplitude of skin SST (K) as a function of daily peak solar radiation (W.m^{-2}), wind speed (m.s^{-1}) and precipitation (mm.h^{-1}).

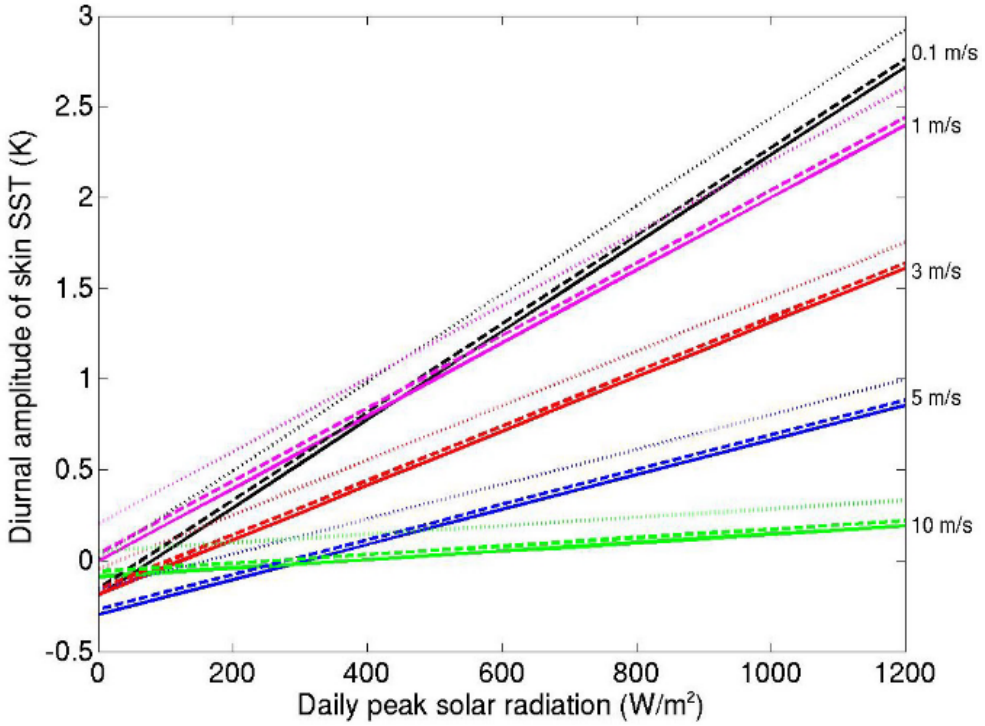

The estimates were obtained by Webster et al. (1996) empirical model. Black, pink, red, blue and green lines represent 0.1, 1, 3, 5 and 10 m.s^{-1} of daily mean wind speed, respectively. The solid, dotted and broken lines represent 0, 1 and 5 mm.h^{-1} of the daily mean precipitation rate.

SOURCE: Kawai e Wada (2007)

To further understand the SST diurnal cycle and how it can be observed, Figure 2.6a

shows an idealized temperature vertical profile. At the first millimetres (0.1-1 mm) of the ocean, a very thin layer called 'cool skin layer' or just 'skin layer' is present both day and night. This layer is thermally stratified (cool water above warm water) due to the intense heat transfer by molecular conduction from the ocean to the atmosphere. Therefore, the 'skin layer' is colder than the layer below, called OML, where the turbulence promotes an almost homogeneous layer. The OML is often stratified under solar heating or precipitation (freshwater flux). In fact, under clear skies and low wind conditions, thermal stratification is established due to solar radiation heating and is called "diurnal warm layer" (FAIRALL et al., 1996), where the SST diurnal cycle is verified. The thermocline that develops near the surface during the day is called "diurnal thermocline" as an indicator of the vertical temperature gradients within the "diurnal warm layer".

Different measures of SST are obtained by satellite infrared sensor, microwave sensor and in situ observations (from ships and buoys), i.e., these instruments estimate the skin, sub-skin and depth (usually 1m) SST, respectively. For this reason, Donlon et al. (2007) defined the following five kinds of SST which are also shown in Figure 2.6b:

a) interface SST (SSTint): shown in grey, the SSTint is a hypothetical temperature that represents the precise temperature at the air-sea interface. SSTint cannot be measured, thus, the SSTskin is used as a reference;

b) skin SST (SSTskin): shown in red, the SSTskin is the temperature at 10-20 μm, i.e., within the molecular conduction layer. It is measured by an infrared radiometer in the band frequency between 3.7-12 μm wavelength (aboard satellites);

c) sub-skin SST (SSTsubskin): shown in pink, SSTsubskin is the temperature at the skin layer base. SSTsubskin is measured by microwave radiometers operating in the band frequency between 6-11 GHz and by high-performance autonomous profilers;

d) sea temperature at depth (SSTdepth): shown in green, SSTdepth is the temperature within the mixed layer. SSTdepth is also mentioned as "bulk" SST. In situ sensors such as thermistor and XBT are used to measure the SSTdepth, usually at about 1m depth;

e) foundation SST (SSTfnd): shown in blue, SSTfnd is the temperature of the water column without the diurnal warming signal (between 5 and 10m),

i.e., similar to the nocturnal SST. SSTfnd is also measured by in situ sensors.

Figure 2.6b, shows a night and day ideal temperature profile resulting from the difference between SSTfnd and the other SST types, hence, the profiles highlight the diurnal warming effect. This effect is important for an accurate estimation of the air-sea fluxes. Therefore, the SST that represents the exact interface between atmosphere and ocean has to be known, however, the SSTskin is considered because SSTint is not measured.

Figure 2.6 - Idealized upper ocean temperature profile (a) and differences between SST and SSTfnd.

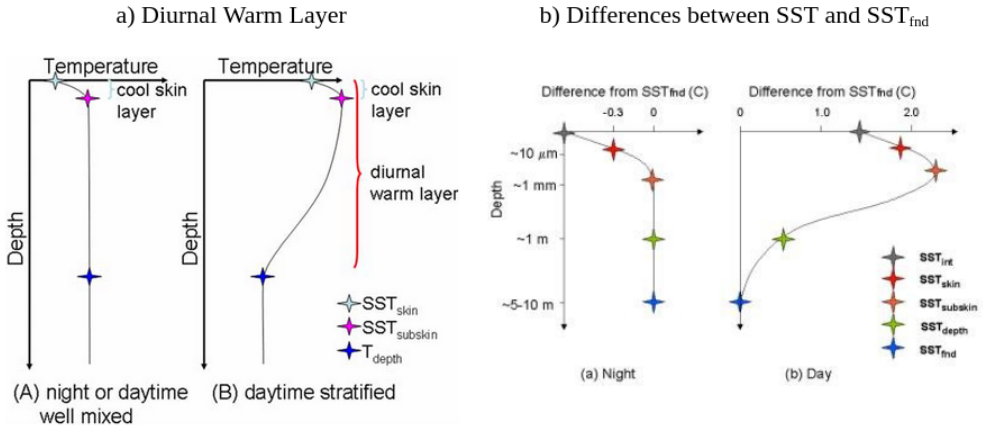

SOURCE: a) Gentemann et al. (2009) and b) Kawai e Wada (2007)

2.5 SST DIURNAL CYCLE OBSERVATIONS

Although the global annual dSST average is 0.1°C, in regions that experience strong incident radiation and weak winds the dSST can reach values higher than 5°C (KAWAI; WADA, 2007). The dSST was first recorded by vessels (SVERDRUP et al., 1942), ocean station data (KOIZUMI, 1956), XBTs (BRUCE; FIRING, 1974), buoys and profiling floats, which measured the SSTdepth, usually at 1m. In these initial studies, it was verified that the mean dSST of 0.2-0.6K varied with latitude and season. Kennedy et al. (2007) obtained a dSST global climatology from 1990 to 2004 using in situ data from hourly drifting buoys shown in Figure 2.7a. Larger dSST values are observed over the tropics but mainly over the western Pacific and the Indian Ocean. The dSST varies with the seasonal maximum insolation following

the summer-hemisphere shown by Figure 2.7b and c. High wind speed decreases the dSST which explains the lower dSST values over mid and high latitudes. More recently, Morak-Bozzo et al. (2016) obtained a longer (1986 to 2012) dSST climatology from drifting buoy data. They verified a strong dSST seasonal, wind speed and cloud cover dependence relation. They were able to show the SST diurnal cycle peak in the early afternoon at 2 pm LT.

Figure 2.7 - Drifting buoy data diurnal SST amplitude from 1990 to 2004.

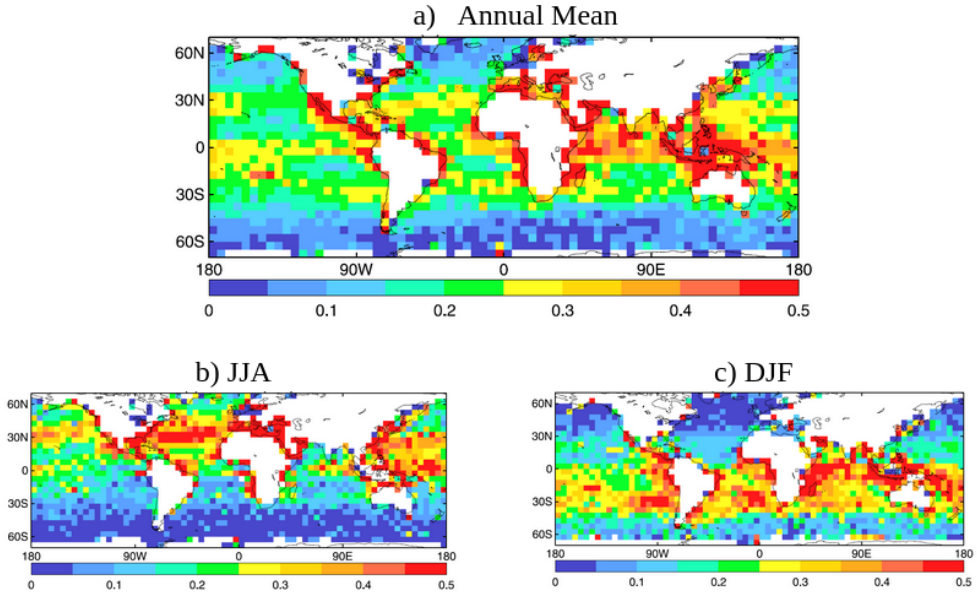

SOURCE: Adapted from Kennedy et al. (2007)

Since the late 1980s, the radiometers and microwave sensors aboard satellites have provided global SST estimates. Through the use of this spatial and temporal data, Stuart-Menteth et al. (2003) using 10 years of infrared data, obtained the first dSST climatology. The authors verified a strong seasonal pattern modulated by wind speed and insolation variations. They observed dSST maximums over the Mediterranean Sea, the Bay of Bengal, Arabian Sea, the seas around Japan, the North Pacific of North America, and the Azores-Bermuda high-pressure belt from spring to summer. These results were consistent with those obtained by Kawai e Wada (2007) using the microwave sensor aboard the Aqua satellite (AMSR-E; Dong et al. (2006), where an improvement was verified over the southern hemisphere.

Although the SST diurnal cycle is important, measuring the SST can be quite chal-

lenging, because each instrument gives a different SST layer measurement (DONLON et al., 2007; GENTEMANN et al., 2009). Therefore, the analysis of the SST data has to consider both application and limitation. The in situ measurements are spatially and temporally limited, and also measure the SST at depths between 25 cm and several metres, it is more suitable for specific areas (KENNEDY et al., 2007). On the other hand, satellite estimated SST data is more suitable for studies that require a greater spatial and temporal coverage (STUART-MENTETH et al., 2003). Even so, some limitations of the abroad satellite sensors must be considered, e.g., infrared sensors are unable to estimate SST under cloudy conditions whereas microwave sensors struggle to gather data under heavy precipitation (KENNEDY et al., 2007).

2.6 SST DIURNAL CYCLE AND AIR-SEA FLUXES

The SST diurnal cycle plays an important role in modulating energy, momentum and mass exchanges between ocean and atmosphere, such as sensible and latent heat and trace gases (KAWAI; WADA, 2007; MOUM; SMYTH, 2001). Accurate SST estimates are important to estimate the air-sea heat fluxes. Webster et al. (1996) verified that an SSTskin error of 1K can lead to a net surface heat flux error of 27 $W.m^{-2}$ in the equatorial western Pacific. Furthermore, Fairall et al. (1996) observed that not representing the diurnal warm layer, can decrease by 20 to 40 $W.m^{-2}$ surface heat flux from the ocean during the daytime. The main effect of the diurnal warm layer is to absorb the incoming solar radiation in the first meters of the ocean surface and increase the heat transfer back to the atmosphere, mainly as latent heat flux (CLAYSON; BOGDANOFF, 2013).

Clayson e Bogdanoff (2013) investigated the effect of diurnal SST variation on air-sea fluxes. They reconstructed an SST diurnal cycle time series using satellite data of wind speed, solar radiation and precipitation. The authors compared estimations of latent and sensible heat fluxes with and without the SST diurnal warming from 1998 to 2007. From a single day analysis, they verified that in the global regions where the diurnal warming reaches 1°C or more, instantaneous errors in H and LE can be greater than $10W.m^{-2}$ and $60W.m^{-2}$, respectively. This result indicates that a surface flux dataset that does not include diurnal warming is incomplete. Furthermore, they verified that both LE and total heat flux spatial seasonal patterns were similar, especially over the tropics, i.e., LE represents 50 to 70% of the total heat flux in the tropics but only 30% in higher latitudes, where H can represent 50%. Figure 2.8 shows the mean 10-years difference between the surface fluxes calculated with and without the SST diurnal cycle. Positive values greater than 5 $W.m^{-2}$ over

the tropical region (between 30ºN and 30°S) indicate that surface fluxes are underestimated when diurnal warming is not considered. In Figure 2.8, major differences are verified over the Indian Ocean, the western equatorial Pacific (warm pool), Indonesia, northwestern Australia and the Mexican west coast. Although the 10-years globally-averaged error in flux calculations was 4.5 W.m^{-2} when the diurnal warming was neglected, over specific regions where the diurnal warming magnitude is greater (shown in Figure 2.8) such as the western tropical Pacific, neglecting the diurnal warming effect led to fluxes errors of 25% to 50%.

Figure 2.8 - 10-year average of the difference between surface fluxes estimated with and without the SST diurnal warming.

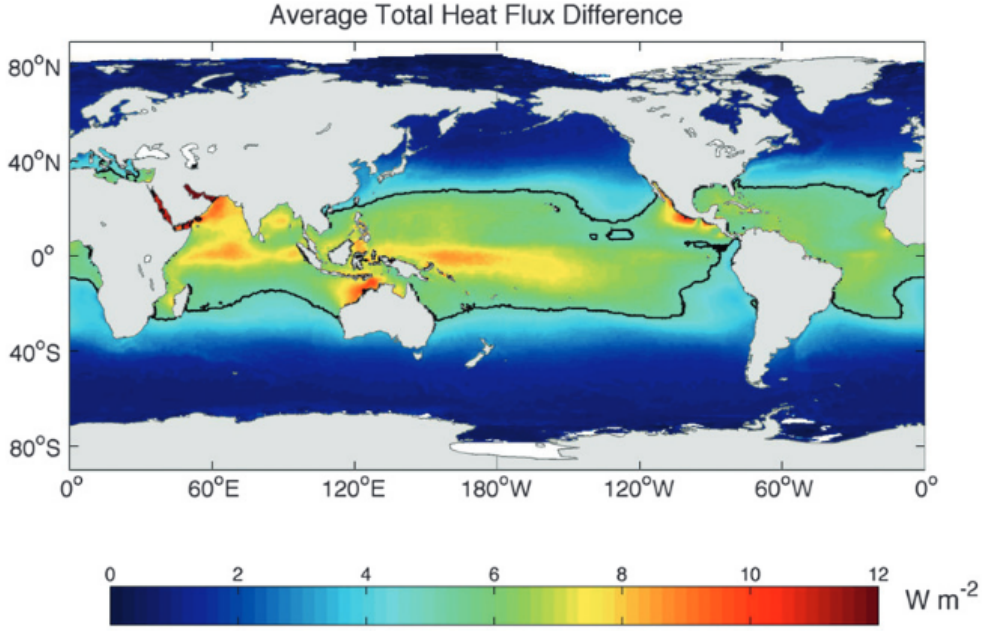

Positive values indicate an underestimation of heat fluxes by non-diurnal SST variation. Contour black lines indicate 5 and 10 W.m^{-2}

SOURCE: Adapted from Clayson e Bogdanoff (2013)

Jeffery et al. (2008) studied the effect of the SST diurnal cycle on air-sea CO_2 flux. In Section 2.3 it is mentioned that equatorial and mid-latitudes are generally CO_2 sources. These areas are also more affected by the diurnal warming variation, i.e, greater SST diurnal cycle magnitude, especially under both low wind and cloud cover (strong insolation) conditions. The authors determined the magnitude of the SST diurnal cycle by a cloud cover and wind speed function and estimated the CO_2 flux. They verified an increase in the gas transfer velocity, thus, in the CO_2 flux

also. Therefore, the SST diurnal cycle related processes are important to improve the CO_2 flux estimates.

The momentum flux is also modified by the diurnal warm layer (DWL) formation because the stable stratification within this layer, inhibits the downward transfer of momentum, i.e, the momentum from wind gets trapped within the DWL (MOULIN et al., 2018). Hughes et al. (2020) studied the horizontal velocity vertical shear evolution when the DWL is formed. They used an idealized numerical simulation to obtain the temperature and velocity shear vertical profiles shown in Figure 2.9. They verified that the DWL induces a near-surface shear shown in Figure 2.9 by the current arrows. The velocity profile at 3pm is coupled with the dSST peak. Furthermore, the OML and the DWL are decoupled due to the stable stratification built up in the DWL. The DWL can induce velocity anomalies forming a diurnal jet, which can increase the near-surface shear by a factor of 5 (SUTHERLAND et al., 2016). However, above a $2 m.s^{-1}$ wind speed threshold, the energy input is sufficient to overcome the stratification and build up instability within the DWL, thus, reducing the velocity shear (HUGHES et al., 2020). Besides, although the diurnal stratification traps the momentum flux from wind within the DWL, the near-surface shear becomes another turbulence source (SUTHERLAND et al., 2016).

Figure 2.9 - DWL induced near-surface velocity shear.

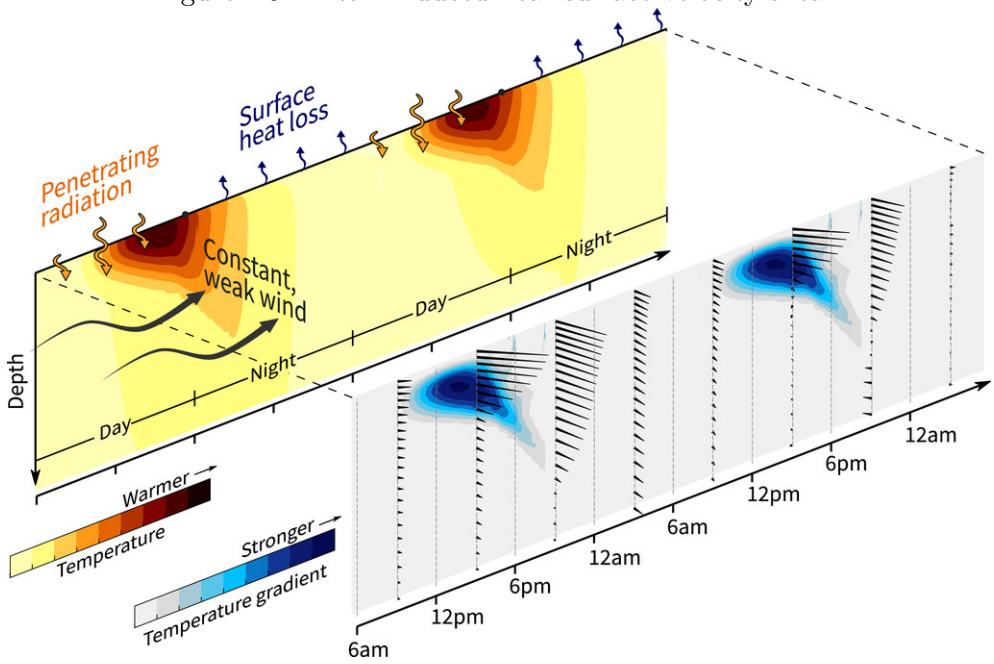

SOURCE: Adapted from Hughes et al. (2020)

2.7 SST DIURNAL CYCLE AND ATMOSPHERIC SYSTEMS

The SST diurnal cycle is affected by meteorological conditions, where a strong SST diurnal cycle is observed under clear skies and weak wind conditions (WEBSTER et al., 1996; WENEGRAT; MCPHADEN, 2015). The energy stored due to diurnal warming is responsible for increase the heat content by 20 $MJ.m^{-2}$ in the first 10 m (MOULIN et al., 2018). This energy can be released to the atmosphere in different time scales. Furthermore, the SST diurnal cycle is important to accurate air-sea fluxes calculations in numerical models (FAIRALL et al., 1996; CLAYSON; BOGDANOFF, 2013). The following studies highlight the importance of resolving or considering the SST diurnal cycle in atmospheric systems, especially over the subseasonal to seasonal time scales.

In the diurnal scale, Kawai et al. (2006) investigated the dSST impact on sea breeze circulation over Mutsu Bay (Japan) and they found that this circulation is weakened in the daytime due to increased upper-ocean warming, i.e., the land-ocean temperature difference decreases. It highlights the need for including the dSST to better simulate the diurnal cycle of convection to improve the land-sea breezes (SLINGO et al., 2003). Johnson et al. (1999) with TOGA-COARE observations verified a strong link between SST and the diurnal cycle of cumulus congestus convection over the western Pacific warm pool. The diurnal cycle peak of convection occurred in the early afternoon when the SST diurnal cycle peak was also verified. The authors suggested that the diurnal cumulus convection is forced by the SST diurnal cycle. Bellenger et al. (2010) used in situ observations to assess the link between SST and convection diurnal cycles over the tropical Indian Ocean. They identified two maximums in the convection diurnal cycle, one in the early morning and the other in the afternoon. The maximum in the afternoon corresponded to days with a diurnal warming layer (dSST), which induced increases in both LE and H that explained 75% of the Convective Inhibition (CIN) decrease. Therefore, the cumulus convection diurnal cycle is driven by SST and surface fluxes variabilities (RUPPERT; JOHNSON, 2016).

Although the dSST involves a diurnal time scale, the amount of energy stored in the OML may interact with intraseasonal time scales (BERNIE et al., 2005; SLINGO et al., 2003). For this reason, Slingo et al. (2003) suggested that the SST diurnal cycle may be a trigger for shallow clouds, playing an important role in Madden Julian Osci (MJO; Zhang (2005)). They verified that during the MJO suppressed phase when the SST diurnal warming is strong, more shallow precipitating clouds are de-

veloped reaching maximum in the early afternoon (near the SST diurnal maximum). The cumulus congestus clouds detrainment promotes gradual moistening of the troposphere, thus, being a precondition to the MJO active phase. This mechanism is called the recharge-discharge (BLADÉ; HARTMANN, 1993), and it was also verified in the composite analysis of Benedict e Randall (2007). Figure 2.10 shows a diagram of the discharge-recharge mechanism in agreement with Benedict e Randall (2007) findings over the eastern Indian and western Pacific Ocean, which the authors chose as the maximum wet phase amplitude and not wave initiation region. First, 10-15 days before deep convection, cumulus convection slowly warms and moistens the low troposphere. During this phase, local forcings associated with LE, moisture convergence and anomalous vertical moisture transport are dominant, supporting the hypothesis that the SST diurnal cycle triggers the cumulus convection. The deep convection and precipitation are active for approximately 10 days. After, the suppressed convection and tropospheric drying associated with anomalous horizontal winds are observed for 20 days.

Figure 2.10 - Diagram of the Discharge-Recharge Mechanism.

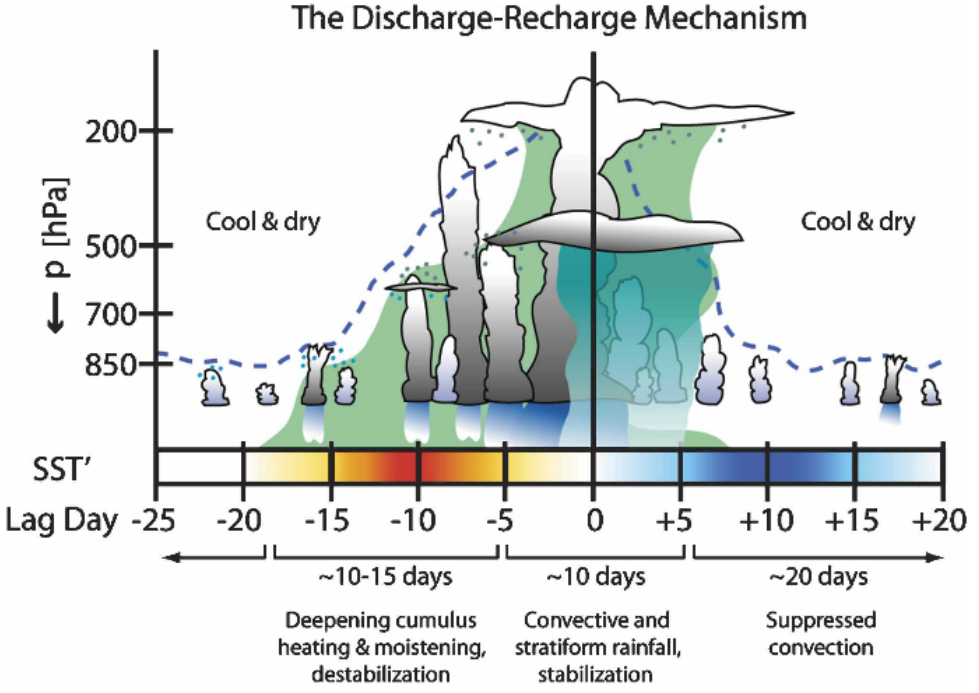

SST' indicates the warm (cold) anomalies in red (blue). The lag days are relative to the maximum rainfall day (day 0). The dashed blue line indicates the approximate cloud top level. Green shading represents when the profile of specific humidity is greater than 0. The detrainment from shallow convective clouds is represented by blue dots.

SOURCE: Adapted from Benedict e Randall (2007)

The importance of the air-sea coupling to MJO has been supported by its improved representation in coupled ocean-atmosphere general circulation models (WOOLNOUGH et al., 2007). The sensitivity experiments of Woolnough et al. (2007) revealed that the improved representation of the SST diurnal cycle was important to improve the representation of MJO. For this reason, Bernie et al. (2005) studied the role of the SST diurnal cycle in MJO using a high resolution 1D vertical mixed layer model. The authors also observed modulation of the dSST during MJO phases, which, during the suppressed phase (low wind speed and high incident solar radiation) the dSST increased. They also suggested that the absence of the SST diurnal may be linked to the weak intraseasonal SST response to MJO in Coupled General Circulation Models (CGCM). This link was later investigated by Bernie et al. (2007), who found that resolving the SST diurnal cycle in a high vertical resolution Ocean General Circulation Model (OCGM), increases by 20% the intraseasonal SST variability across the Indo-Pacific warm pool. Similarly, Guemas et al. (2011) verified that the SST diurnal cycle can affect the intraseasonal variability over the Atlantic Ocean. The authors verified a daily mean SST increase between 0.3 and 0.5°C when the diurnal cycle was represented. The SST correction can persist for 15-40 days over midlatitudes and for more than 60 days in the tropics. It means that the SST correction, also called rectification mechanism due to diurnal warming, can enhance the intraseasonal SST variability by 20-40% over the tropical Atlantic Ocean.

Later, Bernie et al. (2008) performed two 50-year sensitivity experiments: one with ocean-atmosphere general circulation model coupled every 3h and another using daily mean, to assess the impact of resolving the SST diurnal cycle on climate. The dSST inclusion by 3h coupling frequency, increased the climatological SST over the tropics, especially across the tropical Pacific Ocean, where warming of 0.2°C (0.3°C) was verified over central and western (eastern) Pacific. The authors mention that the warming is a consequence of the daily mean SST rectification due to dSST inclusion. Furthermore, this warming promoted a redistribution of precipitation along the Intertropical Convergence Zone (ITCZ) which was displaced towards the equator. A simulation improvement was verified due to dSST inclusion over the western Pacific, where the precipitation between Papua New Guinea and 170°E increased up to 1.22 $mm.day^{-1}$. These changes in SST and precipitation were also consistent with the changes in the surface wind stress, e.g., over the western Pacific, the light winds favored the dSST increase which in turn increases the mean SST and the precipitation. About the MJO, the authors showed precipitation composites, where a stronger and more coherent MJO was verified when the SST diurnal cycle was included. Both MJO propagation and phases were more distinct in the tropical Indo-Pacific. Even

with these improvements, the authors suggest that future improvements in MJO are more likely to come from developments in atmospheric model physics, e.g., parameterizations that represent the diurnal cycle of shallow congestus during the suppressed phase of MJO associated with the recharge-discharge mechanism (BLADÉ; HARTMANN, 1993; BENEDICT; RANDALL, 2007).

The SST diurnal cycle representation increases the SST intraseasonal variability, thus playing an important role in MJO simulation and predictability (BERNIE et al., 2008). To further understand this role, Seo et al. (2014) used a regional ocean-atmosphere coupled model to assess the SST variability effect on the onset and intensity of MJO convection in the Indian Ocean. They performed experiments with 4 different coupling frequencies (CF) for 1 (CF1), 3 (CF3), 6 (CF6) and 24 (CF24) hours, and two not coupled experiments with Weather Research and Forecasting model (WRF): one with prescribed daily-mean SST from CF1 (CF1DM) and other with prescribed persistent SST (CF1PS). The authors verified that during the MJO suppressed phase, more frequent coupling (CF1) results in a stronger SST diurnal cycle, shown in Figure 2.11a, where the black line is observation and the red line is the CF1 experiment. In CF1 (dSST included), the LE diurnal cycle was also stronger and its peak was in the early afternoon shown by the red line Figure 2.11b. The SST diurnal cycle promoted two main effects:

a) time-mean SST and LE increases;

b) enhanced LE diurnal peak, both significant to the convection intensity in the MJO active phase.

Figure 2.11c shows that even though the MJO signal was produced in the experiment without evolving SST (CF1PS), the timing of the peak convection was 1-2 days delayed compared to the experiments with time-varying SST (CF1DM) and with the SST diurnal cycle (CF1). Therefore, the SST diurnal warming during the suppressed phase plays an important role in MJO convection timing mainly through LE contribution to build up the atmospheric moist static energy before and after MJO convection.

The SST diurnal warming is an important heating source that triggers deep convective processes generating wave disturbances in the atmosphere. The MJO convection, for example, is associated with a Kelvin-wave propagation to east and a Rossby-wave that propagates to west (ZHANG, 2005). These atmospheric waves are

Figure 2.11 - SST, LE and precipitation simulations and observations (Revelle, TRMM) during MJO case.

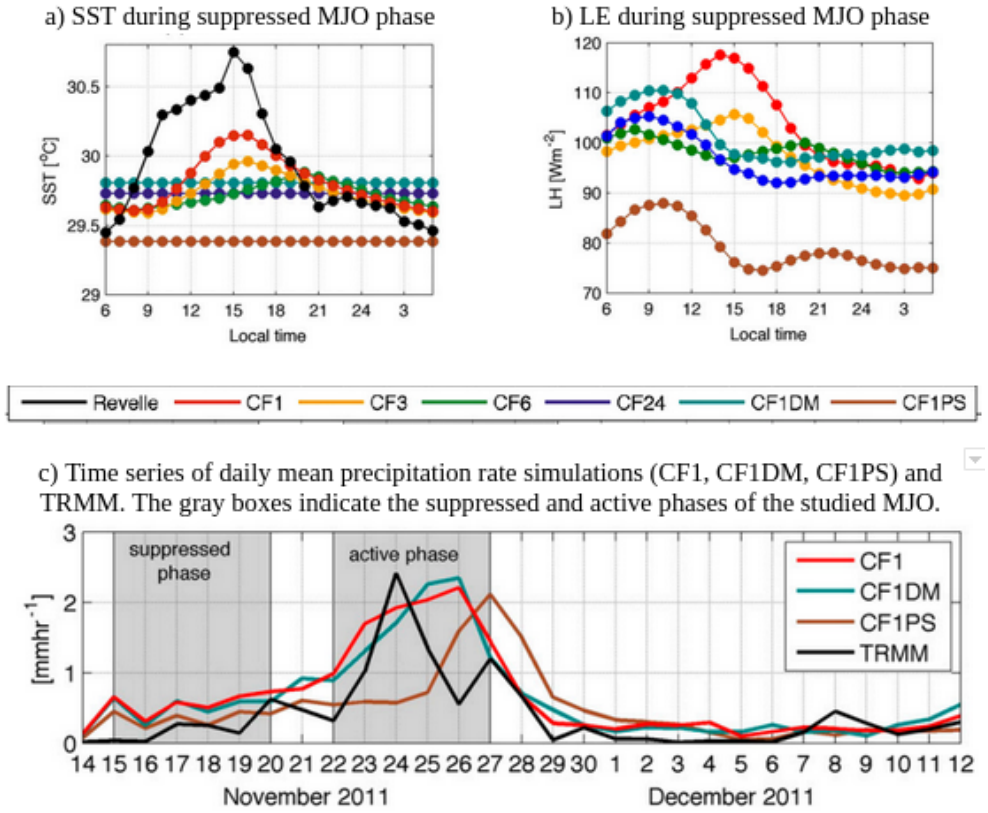

Series are averages over 73-80.5°E 0.7°S-7°N. The LE is positive upward (ocean to atmosphere).

SOURCE: Adapted from Seo et al. (2014)

part of teleconnections and determine the global climate (NIGAM; BAXTER, 2015). The MJO convection propagates eastward over the warm pool from the Indian Ocean to the western Pacific. This eastward propagation was investigated by Stan (2018) who suggested that diurnal to synoptic scales (1-5 days) SST variability impacts the MJO propagation over the Indo-Pacific oceans. They observed that without the high-frequency SST variabilities the MJO convective activity that propagates eastward from the Indian Ocean does not cross Indonesia and the convection in the western Pacific Ocean is locally generated. Tseng et al. (2015) verified that resolving the upper-ocean warm layer improved the intensity, period and propagation speed of MJO. Their study showed that resolving the diurnal warm layer enhances the ocean-atmosphere interaction which intensifies the deep convection and induces a stronger Kelvin-wave perturbation. This means that the eastward propagation mechanism

of the MJO convection is intensified by the SST diurnal cycle. The link between MJO convection, surface fluxes and SST is generally explained by the Air-Sea Convective Intraseasonal Interaction (ASCII; Flatau et al. (1997)) theory (ZHU et al., 2017). Figure 2.12 shows the ASCII conceptual model, where a colder ocean surface is observed at west of the convective cell (C) due to cloud blocking of SWR and strong westerly winds inducing ocean mixing and evaporative fluxes (A). East of the convective cell, weak easterly winds and clear sky conditions contribute to SST increase and to low-level convergence (B). The SST zonal gradient is a surface forcing to build up moist static energy and to develop convection in convergence regions at east of the convective cell. About the above mentioned that the MABL static stability can be forced by SST anomalies, Pezzi et al. (2021) studied how mesoscale oceanic eddies modified both ocean and atmosphere. The authors observed that over a warm core eddy in the Southwestern Atlantic Ocean, the MABL becomes unstable. The authors mentioned the pressure adjustment and the vertical mixing mechanisms. The pressure adjustment involves the establishment of wind convergence over warm core eddies, thus, affects wind, clouds formation and convection, similar to the discussed in ASCII theory. Simultaneously, the vertical mixing mechanism involves the turbulence and wind speed increase over warm waters promoting vertical wind shear reduction which increases the ocean to atmosphere momentum transference and enhances mixing processes in the ocean.

Figure 2.12 - ASCII theory conceptual model.

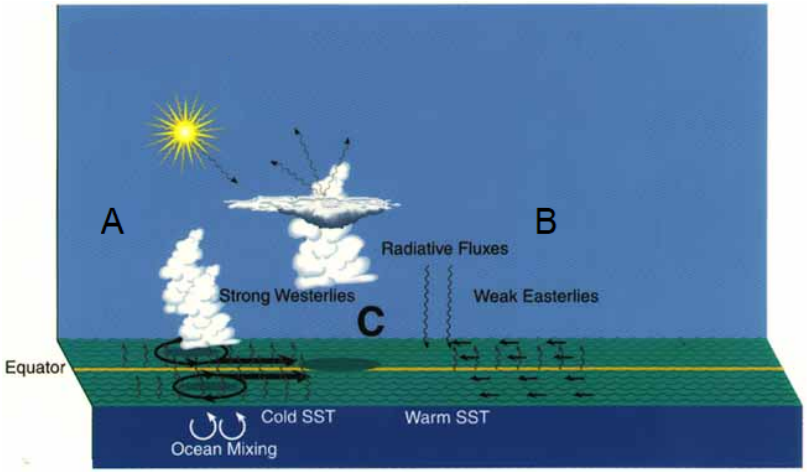

SOURCE: Adapted from Flatau et al. (1997)

The multiscale interactions between high and low-frequency variabilities of the cli-

mate system, explains why the SST diurnal variability can interact with multiple scale atmospheric phenomena (BERNIE et al., 2008). So far, we mentioned the dSST impact on convection and MJO over the tropics, where high values of dSST are observed. However, MJO also interacts with phenomena such as the Asian summer monsoon (PAI et al., 2011) and the El Niño Southern Oscillation (ENSO; Hoell et al. (2014)). In the seasonal scale, Stuart-Menteth et al. (2003) and Mujumdar et al. (2010) verified that the dSST increased over the Bay of Bengal and the South China Sea before the Asian monsoon (boreal spring), suggesting that dSST may affect the monsoon onset. Terray et al. (2012) investigated the impacts of the SST diurnal cycle on coupled phenomena such as the Indian Summer Monsoon (ISM), Indian Ocean Dipole and ENSO. The authors verified a better performance of the experiments coupled every 2 hours and with the high oceanic vertical resolution (301 levels) compared to experiments coupled every 24h to represent ENSO and ISM. The authors argue that this result is associated with the position of the latent heat sources and sinks over the tropical Pacific. However, it is not clear the role of the SST diurnal cycle in these improvements. Zhang et al. (2019) performed forecast experiments forced with hourly, daily and seasonal SST to check their performance on monsoonal events over the Indian Ocean. They did not verify significant differences in the monsoon events whether the atmospheric model is forced with or without the SST diurnal cycle. But, on an ocean-atmosphere coupled model with high vertical resolution in the upper ocean, the prediction skill of the monsoon events was higher. It means that the air-sea interaction processes and the representation of the upper ocean are important to the Indian Monsoon.

ENSO is the main interannual climate variability mode, thus, Masson et al. (2012) investigated the SST intra-daily variability impact on ENSO amplitude. The authors verified a decrease of 15% of ENSO amplitude when the SST intra-daily variability was neglected by the CGCM. However, this change was not associated with the rectification mechanism, which is associated with MJO (BERNIE et al., 2008; GUEMAS et al., 2011). Masson et al. (2012) demonstrated that the intra-daily SST signal was associated with a strengthening of the air-sea feedbacks that are part of the ENSO physics, for example the Bjerknes feedback. This feedback was also mentioned by Tian et al. (2019) to explain the ENSO asymmetry improvement when resolving the intra-daily air-sea interactions by coupling the atmospheric and oceanic model components once per hour. The authors observed that in El Niño events, the SST diurnal cycle anomalies enhanced the atmospheric moist instability, which triggered more convection in the central tropical Pacific. The Bjerknes ocean-atmosphere feedback can be summarized into four characteristics that forms a loop:

a) colder waters over the Pacific east (warmer waters over the Pacific west);

b) stronger SST gradient across the Pacific;

c) enhanced westerly surface winds (trade winds);

d) increased upwelling over Pacific east due to the equatorial upwelling (also caused by the trade winds).

As a loop, any variation in those characteristics has a domino effect. Bjerknes hypothesized that a positive ocean-atmosphere feedback loop causes the ENSO warm phase, i.e, given an positive (negative) SST anomaly over the Pacific east (west), the SST gradient across the Pacific is weakened (also weakens the thermal induced atmospheric circulation known as Walker Circulation), the westerly wind speed is anomalously negative (weaker) and weakens the wind-induced ocean circulation which in turn reduced the upwelling over the Pacific east, also increasing warming of the Pacific east waters. Therefore, Masson et al. (2012) and Tian et al. (2019) showed that improvements in ENSO variability and representation in CGCM can be achieved by a systematic strengthening of the air-sea feedbacks when the SST intra-daily variability is considered.

2.8 MODELING THE SST DIURNAL CYCLE

The studies above highlighted the importance of resolving the SST diurnal cycle to improve the prediction ability of seasonal and subseasonal atmospheric systems. However, most numerical weather and climate models do not consider the SST diurnal variability, either using the daily or monthly mean SST (SALISBURY et al., 2018). In an ocean-atmosphere Coupled General Circulation Model (CGCM) the SST diurnal cycle can be resolved by a better representation of the diurnal warming layer in the Oceanic General Circulation Model (OGCM), which can be achieved by two methods. One involves the direct simulation of the diurnal warming layer by increasing the vertical resolution of the OGCM. In this case, Bernie et al. (2005) verified that a 1m vertical resolution in the upper 100 m of the ocean and 3 hourly or less atmospheric forcing can capture 90% of the dSST. Seo et al. (2014) showed the importance of the coupling frequency (CF), which a 1-hour CF was important to both SST and LE diurnal variations. The limitation of the first method is that it requires many computational resources, which usually is not very practical. The second method involves the use of OML numerical and empirical models in OGCMs. These numerical models with diurnal SST variations can be categorized into three

major groups: diffusion-type, bulk or slab-type and empirical parametric-type models.

The diffusion-type models can either parametrize the turbulent mixing and eddy-diffusion directly by empirical or semi-empirical ways based on Monin-Obukhov similarity theory in the OML (KONDO et al., 1979; LARGE et al., 1994) or estimate turbulence by turbulent closure at each level (MELLOR; YAMADA, 1982).

The bulk or slab-type models assume the OML is a uniform column, i.e., a constant profile of temperature, salinity and velocity. This model type can be further divided into integral and layer models. While the integral represents turbulent mixing at the base of the OML by entrainment, the layer model estimates turbulent kinetic energy in each vertical layer. The latter saves computational resources and it is easier to implement, thus, modifications of the model proposed by Price et al. (1986) also called the PWP model, has been frequently applied to SST diurnal variation studies. The limitation of the PWP model is that it cannot represent the turbulent mixing within the OML, which makes the simulated diurnal SST amplitude (dSST) superior when compared to observations (LARGE et al., 1994; LING et al., 2015). Simplified versions of layer models were developed to avoid high vertical resolution. Fairall et al. (1996) proposed a simplified PWP model that assumes that integrals of surface heat and momentum fluxes are only within the OML, where the temperature profile decreases linearly from surface to bottom, which underestimates the diurnal warming (GENTEMANN et al., 2009). Later, Zeng e Beljaars (2005) developed a prognostic approach to estimate SSTskin, which included a sublayer parameterization in the OGCM under the consideration of a constant sublayer depth and a non-linear temperature decreasing with depth. From a diagnostic approach, Schiller e Godfrey (2005) proposed using the bulk Richardson number (dynamic instability) to estimate the sublayer depth assuming that the temperature within the sublayer is independent of depth.

Lastly, the empirical parametric models estimate the diurnal SST variation from meteorological data, assuming that it primarily depends on wind speed and solar radiation. Stuart-Menteth et al. (2003) estimated the global dSST using Kawai e Kawamura (2002) empirical equations and their results were similar to the dSST from satellite data. Although simple, daily mean meteorological values are necessary to empirical models, making it difficult to use them for prognostic but useful to test the sensitivity of the atmosphere to SST diurnal variations (WEBSTER et al., 1996).

3 FINAL CONSIDERATIONS

Based on the bibliographical review presented in this document about the SST diurnal cycle and its role on seasonal and subseasonal atmospheric systems, the PhD project is going to propose the development of an oceanic surface parametrization that includes the cloud cover and precipitation to represent the SST diurnal cycle. Thus, it is expected to represent the energy propagation from diurnal to subseasonal and seasonal meteorological phenomena, and improve its representation in numerical models.

REFERENCES

ANDRADE, F. M. de; COELHO, C. A.; CAVALCANTI, I. F. Global precipitation hindcast quality assessment of the subseasonal to seasonal (s2s) prediction project models. **Climate Dynamics**, Springer, v. 52, n. 9, p. 5451–5475, 2019. 1

BALAGURU, K.; CHANG, P.; SARAVANAN, R.; LEUNG, L. R.; XU, Z.; LI, M.; HSIEH, J.-S. Ocean barrier layers' effect on tropical cyclone intensification. **Proceedings of the National Academy of Sciences**, National Acad Sciences, v. 109, n. 36, p. 14343–14347, 2012. 8

BELLENGER, H.; TAKAYABU, Y.; USHIYAMA, T.; YONEYAMA, K. Role of diurnal warm layers in the diurnal cycle of convection over the tropical indian ocean during mismo. **Monthly Weather Review**, American Meteorological Society, v. 138, n. 6, p. 2426–2433, 2010. 19

BENEDICT, J. J.; RANDALL, D. A. Observed characteristics of the mjo relative to maximum rainfall. **Journal of the atmospheric sciences**, American Meteorological Society, v. 64, n. 7, p. 2332–2354, 2007. 2, 20, 22

BERNIE, D.; GUILYARDI, E.; MADEC, G.; SLINGO, J.; WOOLNOUGH, S. Impact of resolving the diurnal cycle in an ocean–atmosphere gcm. part 1: A diurnally forced ogcm. **Climate Dynamics**, Springer, v. 29, n. 6, p. 575–590, 2007. 1, 10, 21

BERNIE, D.; GUILYARDI, E.; MADEC, G.; SLINGO, J. M.; WOOLNOUGH, S. J.; COLE, J. Impact of resolving the diurnal cycle in an ocean–atmosphere gcm. part 2: A diurnally coupled cgcm. **Climate dynamics**, Springer, v. 31, n. 7, p. 909–925, 2008. 2, 21, 22, 25

BERNIE, D.; WOOLNOUGH, S.; SLINGO, J.; GUILYARDI, E. Modeling diurnal and intraseasonal variability of the ocean mixed layer. **Journal of climate**, American Meteorological Society, v. 18, n. 8, p. 1190–1202, 2005. 19, 21, 26

BLADÉ, I.; HARTMANN, D. L. Tropical intraseasonal oscillations in a simple nonlinear model. **Journal of Atmospheric Sciences**, v. 50, n. 17, p. 2922–2939, 1993. 20, 22

BRUCE, J.; FIRING, E. Temperature measurements in the upper 10 m with modified expendable bathythermograph probes. **Journal of Geophysical Research**, Wiley Online Library, v. 79, n. 27, p. 4110–4111, 1974. 14

BRUNET, G.; SHAPIRO, M.; HOSKINS, B.; MONCRIEFF, M.; DOLE, R.; KILADIS, G. N.; KIRTMAN, B.; LORENC, A.; MILLS, B.; MORSS, R. et al. Collaboration of the weather and climate communities to advance subseasonal-to-seasonal prediction. **Bulletin of the American Meteorological Society**, American Meteorological Society, v. 91, n. 10, p. 1397–1406, 2010. 1

CHEN, M.; WANG, W.; KUMAR, A. Prediction of monthly-mean temperature: The roles of atmospheric and land initial conditions and sea surface temperature. **Journal of climate**, v. 23, n. 3, p. 717–725, 2010. 1

CHENG, C.-J.; WU, C.-C. The role of wishe in the rapid intensification of tropical cyclones. **Journal of the Atmospheric Sciences**, v. 77, n. 9, p. 3139–3160, 2020. 9

CLAYSON, C. A.; BOGDANOFF, A. S. The effect of diurnal sea surface temperature warming on climatological air–sea fluxes. **Journal of Climate**, American Meteorological Society, v. 26, n. 8, p. 2546–2556, 2013. 2, 16, 17, 19

COELHO, C. A.; SOUZA, D. C. de; KUBOTA, P. Y.; COSTA, S.; MENEZES, L.; GUIMARÃES, B. S.; FIGUEROA, S. N.; BONATTI, J. P.; CAVALCANTI, I. F.; SAMPAIO, G. et al. Evaluation of climate simulations produced with the brazilian global atmospheric model version 1.2. **Climate Dynamics**, Springer, v. 56, n. 3, p. 873–898, 2021. 1

DOBLAS-REYES, F. J.; GARCÍA-SERRANO, J.; LIENERT, F.; BIESCAS, A. P.; RODRIGUES, L. R. Seasonal climate predictability and forecasting: status and prospects. **Wiley Interdisciplinary Reviews: Climate Change**, Wiley Online Library, v. 4, n. 4, p. 245–268, 2013. 1

DONG, S.; GILLE, S. T.; SPRINTALL, J.; GENTEMANN, C. Validation of the advanced microwave scanning radiometer for the earth observing system (amsr-e) sea surface temperature in the southern ocean. **Journal of Geophysical Research: Oceans**, Wiley Online Library, v. 111, n. C4, 2006. 15

DONLON, C.; ROBINSON, I.; CASEY, K.; VAZQUEZ-CUERVO, J.; ARMSTRONG, E.; ARINO, O.; GENTEMANN, C.; MAY, D.; LEBORGNE, P.; PIOLLÉ, J. et al. The global ocean data assimilation experiment high-resolution sea surface temperature pilot project. **Bulletin of the American Meteorological Society**, American Meteorological Society, v. 88, n. 8, p. 1197–1214, 2007. 13, 16

DURACK, P. J.; LEE, T.; VINOGRADOVA, N. T.; STAMMER, D. Keeping the lights on for global ocean salinity observation. **Nature Climate Change**, Nature Publishing Group, v. 6, n. 3, p. 228–231, 2016. 4

EMANUEL, K. A. An air-sea interaction theory for tropical cyclones. part i: Steady-state maintenance. **Journal of Atmospheric Sciences**, v. 43, n. 6, p. 585–605, 1986. 9

FAIRALL, C.; BRADLEY, E. F.; GODFREY, J.; WICK, G.; EDSON, J. B.; YOUNG, G. Cool-skin and warm-layer effects on sea surface temperature. **Journal of Geophysical Research: Oceans**, Wiley Online Library, v. 101, n. C1, p. 1295–1308, 1996. 13, 16, 19, 27

FLATAU, M.; FLATAU, P. J.; PHOEBUS, P.; NIILER, P. P. The feedback between equatorial convection and local radiative and evaporative processes: The implications for intraseasonal oscillations. **Journal of the Atmospheric Sciences**, v. 54, n. 19, p. 2373–2386, 1997. 24

FOLTZ, G. R.; MCPHADEN, M. J. Impact of barrier layer thickness on sst in the central tropical north atlantic. **Journal of Climate**, v. 22, n. 2, p. 285–299, 2009. 8

GENTEMANN, C. L.; MINNETT, P. J.; WARD, B. Profiles of ocean surface heating (posh): A new model of upper ocean diurnal warming. **Journal of Geophysical Research: Oceans**, Wiley Online Library, v. 114, n. C7, 2009. 14, 16, 27

GEORGE, J. V.; VINAYACHANDRAN, P.; VIJITH, V.; THUSHARA, V.; NAYAK, A. A.; PARGAONKAR, S. M.; AMOL, P.; VIJAYKUMAR, K.; MATTHEWS, A. J. Mechanisms of barrier layer formation and erosion from in situ observations in the bay of bengal. **Journal of Physical Oceanography**, American Meteorological Society, v. 49, n. 5, p. 1183–1200, 2019. 8

GRANT, A. L.; BELCHER, S. E. Characteristics of langmuir turbulence in the ocean mixed layer. **Journal of Physical Oceanography**, v. 39, n. 8, p. 1871–1887, 2009. 7

GUEMAS, V.; SALAS-MÉLIA, D.; KAGEYAMA, M.; GIORDANI, H.; VOLDOIRE, A. Impact of the ocean mixed layer diurnal variations on the intraseasonal variability of sea surface temperatures in the atlantic ocean. **Journal of Climate**, v. 24, n. 12, p. 2889–2914, 2011. 21, 25

HARTMANN, D. L. **Global physical climatology**. [S.l.]: Newnes, 2015. 3, 8

HOELL, A.; BARLOW, M.; WHEELER, M. C.; FUNK, C. Disruptions of el niño–southern oscillation teleconnections by the madden–julian oscillation. **Geophysical Research Letters**, Wiley Online Library, v. 41, n. 3, p. 998–1004, 2014. 25

HUGHES, K. G.; MOUM, J. N.; SHROYER, E. L. Evolution of the velocity structure in the diurnal warm layer. **Journal of Physical Oceanography**, v. 50, n. 3, p. 615–631, 2020. 18

JANSSEN, P. A. Ocean wave effects on the daily cycle in sst. **Journal of Geophysical Research: Oceans**, Wiley Online Library, v. 117, n. C11, 2012. 6

JEFFERY, C.; ROBINSON, I.; WOOLF, D.; DONLON, C. The response to phase-dependent wind stress and cloud fraction of the diurnal cycle of sst and air–sea co2 exchange. **Ocean modelling**, Elsevier, v. 23, n. 1-2, p. 33–48, 2008. 17

JOHNSON, R. H.; RICKENBACH, T. M.; RUTLEDGE, S. A.; CIESIELSKI, P. E.; SCHUBERT, W. H. Trimodal characteristics of tropical convection. **Journal of climate**, v. 12, n. 8, p. 2397–2418, 1999. 2, 19

KALNAY, E. **Atmospheric modeling, data assimilation and predictability**. [S.l.]: Cambridge university press, 2003. 1

KARA, A. B.; WALLCRAFT, A. J.; METZGER, E. J.; HURLBURT, H. E.; FAIRALL, C. W. Wind stress drag coefficient over the global ocean. **Journal of climate**, v. 20, n. 23, p. 5856–5864, 2007. 4

KAWAI, Y.; KAWAMURA, H. Evaluation of the diurnal warming of sea surface temperature using satellite-derived marine meteorological data. **Journal of Oceanography**, Springer, v. 58, n. 6, p. 805–814, 2002. 27

KAWAI, Y.; OTSUKA, K.; KAWAMURA, H. Study on diurnal sea surface warming and a local atmospheric circulation over mutsu bay. **Journal of the Meteorological Society of Japan. Ser. II**, Meteorological Society of Japan, v. 84, n. 4, p. 725–744, 2006. 19

KAWAI, Y.; WADA, A. Diurnal sea surface temperature variation and its impact on the atmosphere and ocean: A review. **Journal of oceanography**, Springer, v. 63, n. 5, p. 721–744, 2007. 2, 12, 14, 15, 16

KENNEDY, J. J.; BROHAN, P.; TETT, S. A global climatology of the diurnal variations in sea-surface temperature and implications for msu temperature trends. **Geophysical research letters**, Wiley Online Library, v. 34, n. 5, 2007. 14, 15, 16

KLEIN, S. A.; HARTMANN, D. L. The seasonal cycle of low stratiform clouds. **Journal of Climate**, v. 6, n. 8, p. 1587–1606, 1993. 9

KOIZUMI, M. Researches on the variations of oceanographic conditions in the region of the ocean weather station "extra" in the north pacific ocean (iii) the variation of hydrographic conditions discussed from the heat balance point of view and the heat exchange between sea and atmosphere. **Papers in Meteorology and Geophysics**, Japan Meteorological Agency/Meteorological Research Institute, v. 6, n. 3-4, p. 273–284, 1956. 14

KONDO, J.; SASANO, Y.; ISHII, T. On wind-driven current and temperature profiles with diurnal period in the oceanic planetary boundary layer. **Journal of Physical Oceanography**, v. 9, n. 2, p. 360–372, 1979. 27

LANDSCHÜTZER, P.; LARUELLE, G. G.; ROOBAERT, A.; REGNIER, P. A uniform pco 2 climatology combining open and coastal oceans. **Earth System Science Data**, Copernicus GmbH, v. 12, n. 4, p. 2537–2553, 2020. 4

LARGE, W. G.; MCWILLIAMS, J. C.; DONEY, S. C. Oceanic vertical mixing: A review and a model with a nonlocal boundary layer parameterization. **Reviews of geophysics**, Wiley Online Library, v. 32, n. 4, p. 363–403, 1994. 27

LING, T.; XU, M.; LIANG, X.-Z.; WANG, J. X.; NOH, Y. A multilevel ocean mixed layer model resolving the diurnal cycle: Development and validation. **Journal of Advances in Modeling Earth Systems**, Wiley Online Library, v. 7, n. 4, p. 1680–1692, 2015. 27

LIU, H.; LIN, W.; ZHANG, M. Heat budget of the upper ocean in the south-central equatorial pacific. **Journal of climate**, v. 23, n. 7, p. 1779–1792, 2010. 3

MASSON, S.; TERRAY, P.; MADEC, G.; LUO, J.-J.; YAMAGATA, T.; TAKAHASHI, K. Impact of intra-daily sst variability on enso characteristics in a coupled model. **Climate dynamics**, Springer, v. 39, n. 3, p. 681–707, 2012. 25, 26

MELLOR, G. L.; YAMADA, T. Development of a turbulence closure model for geophysical fluid problems. **Reviews of Geophysics**, Wiley Online Library, v. 20, n. 4, p. 851–875, 1982. 27

MISRA, V. **Regionalizing global climate variations: a study of the Southeastern US regional climate**. [S.l.]: Elsevier, 2020. 8

MORAK-BOZZO, S.; MERCHANT, C.; KENT, E.; BERRY, D.; CARELLA, G. Climatological diurnal variability in sea surface temperature characterized from drifting buoy data. **Geoscience Data Journal**, Wiley Online Library, v. 3, n. 1, p. 20–28, 2016. 15

MOULIN, A. J.; MOUM, J. N.; SHROYER, E. L. Evolution of turbulence in the diurnal warm layer. **Journal of Physical Oceanography**, v. 48, n. 2, p. 383–396, 2018. 18, 19

MOUM, J.; SMYTH, W. Upper ocean mixing. **Encyclopedia of Ocean Sciences**, Academic Press New York, v. 6, p. 3093–3100, 2001. 4, 7, 16

MUJUMDAR, M.; SALUNKE, K.; RAO, S. A.; RAVICHANDRAN, M.; GOSWAMI, B. Diurnal cycle induced amplification of sea surface temperature intraseasonal oscillations over the bay of bengal in summer monsoon season. **IEEE Geoscience and Remote Sensing Letters**, IEEE, v. 8, n. 2, p. 206–210, 2010. 2, 25

NIGAM, S.; BAXTER, S. Teleconnections. encyclopedia of atmospheric sciences, g. north, ed. **Elsevier Science**, v. 90, p. 109, 2015. 23

NORRIS, J. R.; ZHANG, Y.; WALLACE, J. M. Role of low clouds in summertime atmosphere–ocean interactions over the north pacific. **Journal of Climate**, v. 11, n. 10, p. 2482–2490, 1998. 9

PAI, D.; BHATE, J.; SREEJITH, O.; HATWAR, H. Impact of mjo on the intraseasonal variation of summer monsoon rainfall over india. **Climate Dynamics**, Springer, v. 36, n. 1, p. 41–55, 2011. 25

PEZZI, L. P.; SOUZA, R. B. d.; DOURADO, M. S.; GARCIA, C. A. E.; MATA, M.; SILVA-DIAS, M. Ocean-atmosphere in situ observations at the brazil-malvinas confluence region. **Geophysical Research Letters**, Wiley Online Library, v. 32, n. 22, 2005. 4

PEZZI, L. P.; SOUZA, R. B. de; ACEVEDO, O.; WAINER, I.; MATA, M. M.; GARCIA, C. A.; CAMARGO, R. de. Multiyear measurements of the oceanic and atmospheric boundary layers at the brazil-malvinas confluence region. **Journal of Geophysical Research: Atmospheres**, Wiley Online Library, v. 114, n. D19, 2009. 4, 5

PEZZI, L. P.; SOUZA, R. B. de; SANTINI, M. F.; MILLER, A. J.; CARVALHO, J. T.; PARISE, C. K.; QUADRO, M. F.; ROSA, E. B.; JUSTINO, F.; SUTIL, U. A. et al. Oceanic eddy-induced modifications to air–sea heat and co2 fluxes in the brazil-malvinas confluence. **Scientific reports**, Nature Publishing Group, v. 11, n. 1, p. 1–15, 2021. 24

PRICE, J. F.; WELLER, R. A.; PINKEL, R. Diurnal cycling: Observations and models of the upper ocean response to diurnal heating, cooling, and wind mixing. **Journal of Geophysical Research: Oceans**, Wiley Online Library, v. 91, n. C7, p. 8411–8427, 1986. 27

ROBERTSON, A. W.; KUMAR, A.; PEÑA, M.; VITART, F. Improving and promoting subseasonal to seasonal prediction. **Bulletin of the American Meteorological Society**, v. 96, n. 3, p. ES49–ES53, 2015. 1

ROSA, E. B. **Variabilidade submensal da camada de mistura marinha durante episódios de ZCAS oceânica**. 81 p. Tese (Doutorado) — Instituto Nacional de Pesquisas Espaciais (INPE), São José dos Campos, 2021-08-19 2022. Disponível em: <http://urlib.net/ibi/8JMKD3MGP3W34T/45NDUHB>. Acesso em: 12 maio 2022. 8

RUPPERT, J. H.; JOHNSON, R. H. On the cumulus diurnal cycle over the tropical warm pool. **Journal of Advances in Modeling Earth Systems**, Wiley Online Library, v. 8, n. 2, p. 669–690, 2016. 19

SALISBURY, D.; MOGENSEN, K.; BALSAMO, G. **Use of in situ observations to verify the diurnal cycle of sea surface temperature in ECMWF coupled model forecasts**. [S.l.]: European Centre for Medium Range Weather Forecasts, 2018. 2, 26

SCHILLER, A.; GODFREY, J. A diagnostic model of the diurnal cycle of sea surface temperature for use in coupled ocean-atmosphere models. **Journal of Geophysical Research: Oceans**, Wiley Online Library, v. 110, n. C11, 2005. 27

SEO, H.; SUBRAMANIAN, A. C.; MILLER, A. J.; CAVANAUGH, N. R. Coupled impacts of the diurnal cycle of sea surface temperature on the madden–julian oscillation. **Journal of Climate**, v. 27, n. 22, p. 8422–8443, 2014. 2, 22, 23, 26

SHUKLA, J. Predictability in the midst of chaos: A scientific basis for climate forecasting. **science**, American Association for the Advancement of Science, v. 282, n. 5389, p. 728–731, 1998. 1

SLINGO, J.; INNESS, P.; NEALE, R.; WOOLNOUGH, S.; YANG, G. Scale interactions on diurnal toseasonal timescales and their relevanceto model systematic errors. **Annals of Geophysics**, v. 46, n. 1, 2003. 2, 19

STAN, C. The role of sst variability in the simulation of the mjo. **Climate Dynamics**, Springer, v. 51, n. 7, p. 2943–2964, 2018. 2, 23

STEFFEN, W.; RICHARDSON, K.; ROCKSTRÖM, J.; SCHELLNHUBER, H. J.; DUBE, O. P.; DUTREUIL, S.; LENTON, T. M.; LUBCHENCO, J. The emergence and evolution of earth system science. **Nature Reviews Earth & Environment**, Nature Publishing Group, v. 1, n. 1, p. 54–63, 2020. 3

STUART-MENTETH, A. C.; ROBINSON, I. S.; CHALLENOR, P. G. A global study of diurnal warming using satellite-derived sea surface temperature. **Journal of Geophysical Research: Oceans**, Wiley Online Library, v. 108, n. C5, 2003. 15, 16, 25, 27

SUTHERLAND, G.; MARIÉ, L.; REVERDIN, G.; CHRISTENSEN, K. H.; BROSTRÖM, G.; WARD, B. Enhanced turbulence associated with the diurnal jet in the ocean surface boundary layer. **Journal of Physical Oceanography**, v. 46, n. 10, p. 3051–3067, 2016. 18

SVERDRUP, H. U.; JOHNSON, M. W.; FLEMING, R. H. et al. **The Oceans: Their physics, chemistry, and general biology**. [S.l.]: Prentice-Hall New York, 1942. 9, 14

TAKAHASHI, T.; SUTHERLAND, S. C.; WANNINKHOF, R.; SWEENEY, C.; FEELY, R. A.; CHIPMAN, D. W.; HALES, B.; FRIEDERICH, G.; CHAVEZ, F.; SABINE, C. et al. Climatological mean and decadal change in surface ocean pco2, and net sea–air co2 flux over the global oceans. **Deep Sea Research Part II: Topical Studies in Oceanography**, Elsevier, v. 56, n. 8-10, p. 554–577, 2009. 4

TALLEY, L. D. **Descriptive physical oceanography: an introduction**. [S.l.]: Academic press, 2011. 5, 7

TERRAY, P.; KAMALA, K.; MASSON, S.; MADEC, G.; SAHAI, A.; LUO, J.-J.; YAMAGATA, T. The role of the intra-daily sst variability in the indian monsoon variability and monsoon-enso–iod relationships in a global coupled model. **Climate dynamics**, Springer, v. 39, n. 3, p. 729–754, 2012. 2, 25

TIAN, F.; STORCH, J.-S. v.; HERTWIG, E. Impact of sst diurnal cycle on enso asymmetry. **Climate Dynamics**, Springer, v. 52, n. 3, p. 2399–2411, 2019. 25, 26

TRENBERTH, K. Earth system processes. **Encyclopedia of global environmental change**, Citeseer, v. 2, p. 13–30, 2002. 3

TSENG, W.-L.; TSUANG, B.-J.; KEENLYSIDE, N. S.; HSU, H.-H.; TU, C.-Y. Resolving the upper-ocean warm layer improves the simulation of the madden–julian oscillation. **Climate Dynamics**, Springer, v. 44, n. 5, p. 1487–1503, 2015. 23

VITART, F.; ROBERTSON, A. W.; ANDERSON, D. L. Subseasonal to seasonal prediction project: Bridging the gap between weather and climate. **Bulletin of the World Meteorological Organization**, v. 61, n. 2, p. 23, 2012. 1

WEBSTER, P. J.; CLAYSON, C. A.; CURRY, J. A. Clouds, radiation, and the diurnal cycle of sea surface temperature in the tropical western pacific. **Journal of Climate**, v. 9, n. 8, p. 1712–1730, 1996. 11, 16, 19, 27

WENEGRAT, J. O.; MCPHADEN, M. J. Dynamics of the surface layer diurnal cycle in the equatorial atlantic ocean (0, 23 w). **Journal of Geophysical Research: Oceans**, Wiley Online Library, v. 120, n. 1, p. 563–581, 2015. 10, 11, 19

WOOLNOUGH, S.; VITART, F.; BALMASEDA, M. The role of the ocean in the madden–julian oscillation: Implications for mjo prediction. **Quarterly Journal of the Royal Meteorological Society: A journal of the atmospheric sciences, applied meteorology and physical oceanography**, Wiley Online Library, v. 133, n. 622, p. 117–128, 2007. 1, 21

ZENG, X.; BELJAARS, A. A prognostic scheme of sea surface skin temperature for modeling and data assimilation. **Geophysical Research Letters**, Wiley Online Library, v. 32, n. 14, 2005. 27

ZHANG, C. Madden-julian oscillation. **Reviews of Geophysics**, Wiley Online Library, v. 43, n. 2, 2005. 1, 19, 22

ZHANG, Y.; HUNG, M.-P.; WANG, W.; KUMAR, A. Role of sst feedback in the prediction of the boreal summer monsoon intraseasonal oscillation. **Climate Dynamics**, Springer, v. 53, n. 7, p. 3861–3875, 2019. 2, 25

ZHONGMING, Z.; LINONG, L.; XIAONA, Y.; WANGQIANG, Z.; WEI, L. et al. Ar6 climate change 2021: The physical science basis. 2021. 4

ZHU, J.; WANG, W.; KUMAR, A. Simulations of mjo propagation across the maritime continent: Impacts of sst feedback. **Journal of Climate**, v. 30, n. 5, p. 1689–1704, 2017. 24

PUBLICAÇÕES TÉCNICO-CIENTÍFICAS EDITADAS PELO INPE

Teses e Dissertações (TDI)

Teses e Dissertações apresentadas nos Cursos de Pós-Graduação do INPE.

Notas Técnico-Científicas (NTC)

Incluem resultados preliminares de pesquisa, descrição de equipamentos, descrição e ou documentação de programas de computador, descrição de sistemas e experimentos, apresentação de testes, dados, atlas, e documentação de projetos de engenharia.

Propostas e Relatórios de Projetos (PRP)

São propostas de projetos técnico-científicos e relatórios de acompanhamento de projetos, atividades e convênios.

Publicações Seriadas

São os seriados técnico-científicos: boletins, periódicos, anuários e anais de eventos (simpósios e congressos). Constam destas publicações o Internacional Standard Serial Number (ISSN), que é um código único e definitivo para identificação de títulos de seriados.

Pré-publicações (PRE)

Todos os artigos publicados em periódicos, anais e como capítulos de livros.

Manuais Técnicos (MAN)

São publicações de caráter técnico que incluem normas, procedimentos, instruções e orientações.

Relatórios de Pesquisa (RPQ)

Reportam resultados ou progressos de pesquisas tanto de natureza técnica quanto científica, cujo nível seja compatível com o de uma publicação em periódico nacional ou internacional.

Publicações Didáticas (PUD)

Incluem apostilas, notas de aula e manuais didáticos.

Programas de Computador (PDC)

São a seqüência de instruções ou códigos, expressos em uma linguagem de programação compilada ou interpretada, a ser executada por um computador para alcançar um determinado objetivo. Aceitam-se tanto programas fonte quanto os executáveis.